Model-Driven Quantization for Time Encoding Machines

Dorian Florescu
Department of Electrical and Electronic Engineering
Imperial College London
South Kensington, SW7 2AZ London, U.K.
Email: d.florescu@imperial.ac.uk

***Abstract*—In conventional analog-to-digital (ADC) conversion, the sampling and quantization steps take place on the time and amplitude axes, respectively. In the case of time encoding machines (TEMs), which convert analog signals into a sequence of time events, sampling and quantization interfere with one another since they both operate on the time axis. Here we introduce a new quantization method for TEMs called QTEM that, due to its model-driven nature, limits the interference of sampling and quantization. We show that existing recovery guarantees don't apply to QTEM. We provide new guarantees for recovering the input of the QTEM and demonstrate numerically its advantage over conventional TEM quantization.**

I. Introduction

Analog-to-digital conversion (ADC) is generally characterized as a two-step process: 1) discretization of the time axis – sampling, and 2) discretization of the amplitude axis – quantization [1]. Besides allowing the storage and processing on a computer, the resulted digital signal also has increased transmission robustness. Unlike traditional ADCs that encode information on the amplitude axis, the time encoding machines (TEMs) transmit pulses in an asynchronous fashion, thus encoding the information solely on the time axis. The TEMs are particularly attractive for their low-power transmission properties, inspired from the biological nervous system [2]. The input recovery approach, known as a Time Decoding Machine (TDM) has been realised for the case of bandlimited inputs [2]–[4], inputs belonging to shift-invariant spaces [4], [5], and also inputs with jump discontinuities [6]–[8]. The study of TEMs in the presence of noise was considered in [2], [9]–[12].

Motivation. Despite functioning only in the time domain, the digitization process of time encoded signals [2] remains a two-step process: sampling (generating the TEM signal), and quantization (modelled as uniform jitter noise). Unlike conventional ADCs, here each step acts sequentially in the time domain partially diminishing the other step's contribution. The trade-off between quantization and sampling is well understood for conventional ADCs. Given that quantization can be modelled as uniform bounded noise, the distortion introduced can be partly reduced via a higher sampling rate. For time encoding, however, a higher sampling rate brings samples closer in time, which makes them more sensitive to quantization jitter. Even though quantization was studied before for time encoding [2], [13]–[18], there are still remaining unknowns. For example, it is unclear how one can compensate for quantization noise via a higher sampling rate. Moreover, given that both sampling and quantization happen in the time domain, it would be desirable to be implemented both in one operation where the practical setup allows it.

Contributions. Here we introduce a new model-driven quantization method for TEMs, called quantized TEM (QTEM), for an asynchronous sigma-delta modulator (ASDM) TEM. We show that the output of the QTEM cannot be modeled via conventional quantization, therefore existing recovery methods are not applicable. Theoretically, we show that QTEM amounts to projecting the input onto a discrete sequence depending on the QTEM parameters and a bounded noise sequence. Using frame theory, we prove that the input can be recovered from its projections if a density criterion is satisfied. We show that the proposed QTEM leads to better input reconstructions than the conventional quantization using extensive numerical simulations.

This research is supported by the UK Research and Innovation council's Future Leaders Fellowship program "Sensing Beyond Barriers" (MRC Fellowship award no. MR/S034897/1). Further details on Unlimited Sensing and upcoming materials on *reproducible research* are available via `https://bit.ly/USF-Link`.

II. The Time Encoding Machine

A TEM with continuous-time input $g^c(t)$ is an operator $\mathcal{T}$ defined as $\mathcal{T}g^c = \{t_k\}_{k\in\mathbb{Z}}$, where $\{t_k\}_{k\in\mathbb{Z}}$ is a strictly increasing sequence. Here we consider the case of an Asynchronous Sigma-Delta Modulator (ASDM) TEM, characterised by low power consumption [19] and modular design [20]. The ASDM was used as an alternative to conventional ADCs in [21] and also included in applications such as brain-machine interfaces [22]. The ASDM consists of a loop with an adder, integrator, and a noninverting Schmitt trigger (Fig. 2). For initial condition $z(0) = -b$, $\{t_n\}_{n\geqslant 1}$ satisfy the t-transform equations

$$\int_{t_k}^{t_{k+1}} g^c(s)ds = (-1)^k \left[2\delta - b(t_{k+1} - t_k)\right], \qquad (1)$$

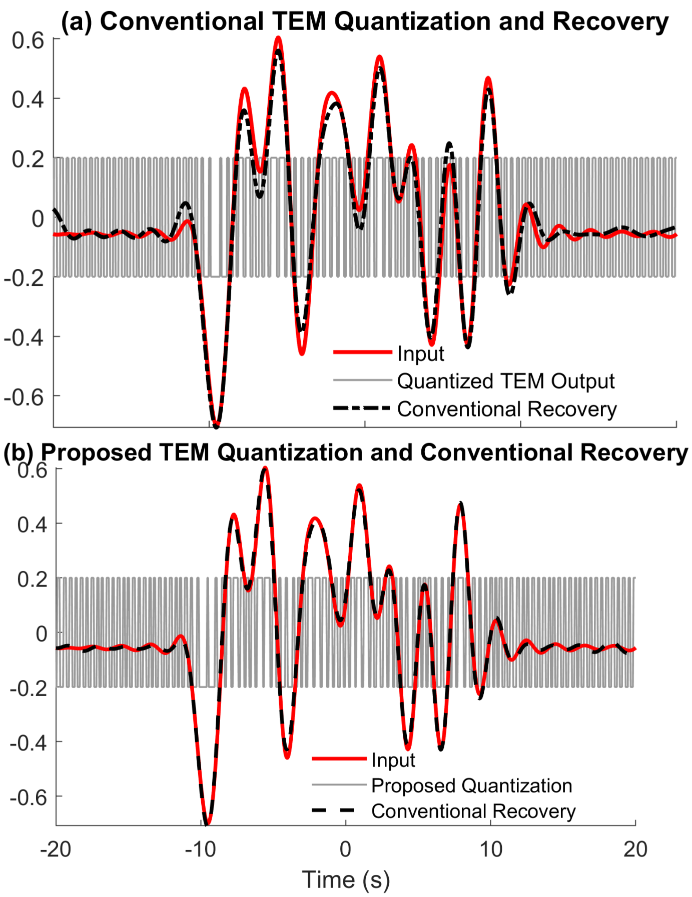

Figure 1: Comparative reconstruction performance for the (a) conventional and (b) proposed quantization of an ASDM output.

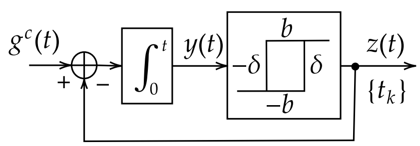

Figure 2: The asynchronous sigma-delta modulator (ASDM).

where $\delta, b > 0$ are the ASDM parameters. We assume $g^c \in \mathsf{PW}_\pi$, where PW_π is the Paley-Winer space of bandwidth Ω

$$\mathsf{PW}_\pi = \left\{ g^c \in L^2(\mathbb{R}) \, | \mathcal{F} g^c \subseteq [-\pi, \pi] \right\},$$

where $L^2(\mathbb{R})$ is the space of square integrable functions. Furthermore, we assume $|g^c(t)| \leqslant c < b, c > 0$. Then [2]

$$\frac{2\delta}{b+c} \leqslant \Delta t_n \leqslant \frac{2\delta}{b-c}. \quad (2)$$

If the TEM output satisfies the Nyquist rate condition $|t_{k+1} - t_k| < 1$, sufficiently guaranteed by $2\delta < b - c$ (2), then $g^c(t)$ is uniquely identified by $\{t_k\}_{k\in\mathbb{Z}}$ [2]. We next review the conventional quantization for TEM outputs.

III. Conventional Quantization for Time Encoding Machines

Here, the samples $\{t_k\}_{k\in\mathbb{Z}}$ are quantized with resolution T, leading to $\{t_k^q\}_{k\in\mathbb{Z}}$ such that $|t_k^q - t_k| < T/2$. This can be done by quantizing the absolute sample as $t_k^q = T \cdot \text{round}\left(\frac{t_k}{T}\right)$,

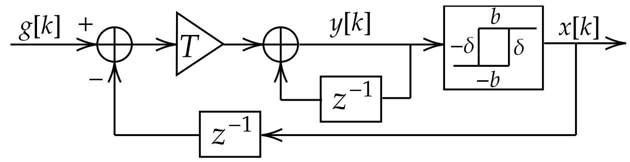

Figure 3: The proposed quantized TEM circuit.

where round is the function rounding to the nearest integer. The quantized samples are then transmitted through a channel. We model the effect of the channel as jitter noise sequence η_k such that the channel output is given by $\widetilde{t}_k^q = t_k^q + \eta_k$. If $|\eta_k| < T$, then the effect of the jitter can be fully eliminated by exploiting the quantized structure of the samples, thus acquiring t_k^q. At the receiver end, the input recovery is

$$\widetilde{g}^c(t) = \sum\nolimits_{m\in\mathbb{Z}} \widetilde{c}_m \cdot \text{sinc}\,(t-m),$$

where $\text{sinc}\,(t) \triangleq \frac{\sin(\pi \cdot t)}{\pi \cdot t}$ and coefficients $\widetilde{c}_k$ are the solution in the least square sense of the following system.

$$\sum_{n\in\mathbb{Z}} c_n \int_{t_k^q}^{t_{k+1}^q} \text{sinc}\,(t-n)\, dt \simeq 2(-1)^k \delta - (-1)^k b \Delta t_k^q. \quad (3)$$

IV. Proposed Quantization Method

The key idea is to exploit the knowledge of T during TEM encoding. We assume $T = 1/N$, where $N \in \mathbb{Z}_+^*$. Let $g[l] = g^c\left(\frac{l}{N}\right)$ and assume $|g[l]| \leqslant c < b$. The proposed TEM quantization (QTEM) model is an operator $\mathcal{T}^q g^c = \{t_k^{q_2}\}_{k\in\mathbb{Z}} = \{n_k T\}_{k\in\mathbb{Z}}$, depicted in Fig. 3, such that

$$y[k] = \sum\nolimits_{l=1}^{k} T(g[l] - x[l-1]) + Tg[0], k \in \mathbb{Z}. \quad (4)$$

Assuming $x[0] = -b$, $y[0] = 0$ we have $y[1] = Tg[0]$ and, as long as $y[k-1] \leqslant \delta, k \geqslant 2$, we have $x[k-1] = -b$ and thus $y[k]$ is strictly increasing, given that $|g[l]| < b$. This means that eventually $y[k] > \delta$ for $k = n_1 + 1$, which flips the output to $x[n_1+1] = b$. Next, sequence $y[k]$ becomes strictly decreasing, and the output flips again to $-b$ when $y[k]$ crosses $-\delta$ for $k = n_2 + 1$. We note that, due to the discrete nature of the QTEM, the thresholds $\pm\delta$ are generally never reached exactly, but directly exceeded, as opposed to the ASDM in Section II. We define the output of the QTEM as the time samples $t_k^{q_2} = n_k T$ located right before $\pm\delta$ is crossed, defined by the discrete-time *t-transform* equations

$$T \sum\nolimits_{l=0}^{n_k} g[l] = y[n_k] + T \sum\nolimits_{l=0}^{n_k - 1} x[l] \simeq (-1)^{k+1}\delta. \quad (5)$$

We note that the principle underlying the proposed QTEM could be used as an approximation of a TEM on a digital computer. However, in this latter case, the purpose is to make T negligible to achieve the best possible approximation, which is a different problem than considered in this manuscript. The next lemma enables bounding the QTEM output density.

Lemma 1. *Let $\{n_k T\}_{k\in\mathbb{Z}}$ be the set of switching times generated by a QTEM with bounded input $|g[k]| < c$ for a quantization step T and parameters δ, b. Then*

$$\frac{2\delta}{b+c} < Tn_{k+1} - Tn_k \leqslant \frac{2\delta}{b-c}. \quad (6)$$

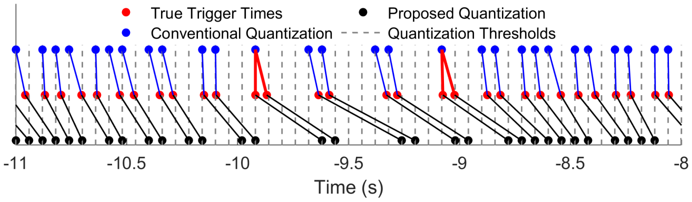

Figure 4: Proposed QTEM vs conventionally quantized TEM.

Lemma 1 proves the discrete version of ASDM bounds (2). Moreover, we note that the lower bound in (6) is strict and thus $Tn_{k+1} > Tn_k, \forall k \in \mathbb{Z}$, meaning that the switching times never overlap. This is not a guarantee for conventional quantization (see Fig. 4). Using (4) and (5) we get that

$$\begin{aligned} \left|y_{n_k} - (-1)^{k+1}\delta\right| \leqslant |\Delta y_{n_k}| = T\,|g_{n_k} - x_{n_k-1}| \\ \leqslant T(b+c), \quad \forall k \in \mathbb{Z}. \end{aligned} \tag{7}$$

We note that the RHS of (5) is known with precision $T(b+c)$ (7) which can be made arbitrarily small by increasing the quantization resolution. In fact, it can be shown that $\lim_{T\to 0} t_k^{q_2} = t_k, \quad \forall k \in \mathbb{Z}$. Despite this, when $T \gg 0$, the output of the QTEM can be considerably different to the output of the TEM. Moreover, unlike conventional TEM quantization, the relationships $|t_k^{q_2} - t_k| < T$ or $|\Delta t_k^{q_2} - \Delta t_k| < T$ do not necessarily hold true, which is also the case in Fig. 4. Therefore, the existing recovery guarantees for TEMs with and without quantization are not directly applicable for the QTEM [2]. In the following we derive the input recovery conditions.

V. QTEM Input Recovery

We note that (5) can be re-written as

$$T\sum\nolimits_{l=n_k+1}^{n_{k+1}} g[l] = 2(-1)^k\delta + T\sum\nolimits_{l=n_k+1}^{n_{k+1}-1} x[l] + \varepsilon_k, \tag{8}$$

where $\varepsilon_k \triangleq y\left[n_{k+1}\right] - y\left[n_k\right] - 2(-1)^k\delta$. Note that in the RHS of (8) the only unknown is ε_k, which is treated as a sequence of bounded noise satisfying $|\varepsilon_k| \leqslant 2T(b+c)$ (7). Therefore, we first consider that we know $T\sum_{l=n_k+1}^{n_{k+1}} g[l]$, and later on analyse the effect of ε_k. From (8)

$$T \cdot \langle g, \mathbb{1}_{[n_k+1, n_{k+1}]}\rangle_{\ell^2} = d_k, \tag{9}$$

where $\mathbb{1}_S(k), k \in \mathbb{Z}$ is the indicator function of set S, $\langle\cdot,\cdot\rangle_{\ell^2}$ is the standard inner product in ℓ^2 and $d_k = 2(-1)^k\delta + T\sum_{l=n_k+1}^{n_{k+1}-1} x[l] + \varepsilon_k$ is considered a known sequence. The problem proposed is to recover the input from $\{d_k\}_{k\in\mathbb{Z}}$. The next theorem proves that sequence d_k uniquely identifies samples $g[l]$ and consequently continuous-time function $g^c(t)$.

Theorem 1 (Unique Representation)**.** *Let $g[l]$ be samples acquired at rate $N = \frac{1}{T} \in \mathbb{Z}_+^*$ from $g^c \in \mathsf{PW}_\pi$, $|g^c(t)| < c$, such that $g[l] = g^c\left(\frac{l}{N}\right)$. Let $t_k^{q_2} = n_k T$ be the output switching times of a QTEM with parameters δ, b, in response to input $g[l]$. If $b > c$ and $\delta < \frac{b-c}{4}$, then $g[l]$ and $g^c(t)$ are uniquely represented by $d_k = T \cdot \langle g, \mathbb{1}_{[n_k+1, n_{k+1}]}\rangle_{\ell^2}, k \in \mathbb{Z}$.*

Proof. Since $g^c \in \mathsf{PW}_\pi$, then $\{g^c(l)\}_{l\in\mathbb{Z}} \subseteq \ell^2$, where $\ell^2 = \left\{a \in \mathbb{R}^\infty \;\middle|\; \sum_{l\in\mathbb{Z}} a_l^2 < \infty\right\}$. When oversampling by $N \in \mathbb{Z}_+^*$, $g[l] = g^c\left(\frac{l}{N}\right)$ no longer span all ℓ^2, but rather a subspace ℓ_N^2 defined by

$$\ell_N^2 = \operatorname{span}\left\{h_l, l \in \mathbb{Z}\right\}, h_l[k] \triangleq N^{-\frac{1}{2}} \cdot \operatorname{sinc}\left(k/N - l\right), \tag{10}$$

for $k \in \mathbb{Z}$. It can be directly proven that ℓ_N^2 is a Hilbert space with inner product $\langle\cdot,\cdot\rangle_{\ell^2}$ and orthonormal basis functions h_l such that $\langle h_l, h_m\rangle_{\ell^2} = \mathbb{1}_{\{m\}}(l)$. Moreover, for two sequences $g[l] = g^c\left(\frac{l}{N}\right)$, $\bar{g}[l] = \bar{g}^c\left(\frac{l}{N}\right)$ due to Parseval we get that

$$\langle g, \bar{g}\rangle_{\ell^2} = N \cdot \langle g^c, \bar{g}^c\rangle_{L^2}, \quad \|g\|_{\ell^2} = N \cdot \|g^c\|_{L^2}. \tag{11}$$

Generally $\mathbb{1}_{[n_k+1, n_{k+1}]} \notin \ell_N^2$. Via the inner product linearity,

$$\begin{aligned} \langle g, \mathbb{1}_{[n_k+1,n_{k+1}]}\rangle_{\ell^2} &= \langle g, \psi_k\rangle_{\ell^2} + \langle g, \mathcal{P}_{\ell^2\setminus\ell_N^2}\mathbb{1}_{[n_k+1,n_{k+1}]}\rangle_{\ell^2} \\ &= \langle g, \psi_k\rangle_{\ell^2}, \end{aligned}$$

where $\psi_k = \mathcal{P}_{\ell_N^2}\mathbb{1}_{[n_k+1,n_{k+1}]}$ and $\mathcal{P}_{\mathbb{S}}$ represents the projection operator onto space $\mathbb{S}$. We use that $g \in \ell_N^2$ and thus its projection outside this space is 0. We compute ψ_k as

$$\psi_k[n] = \sum_{l\in\mathbb{Z}} \langle \mathbb{1}_{[n_k+1,n_{k+1}]}, h_l[m]\rangle_{\ell^2} \cdot h_l[n] \tag{12}$$

$$= \sum_{l\in\mathbb{Z}}\sum_{m=n_k+1}^{n_{k+1}} h_l[m]\cdot h_l[n] = \frac{1}{N}\sum_{m=n_k+1}^{n_{k+1}} I_m[n], \tag{13}$$

where $I_m[n] = \sum_{l\in\mathbb{Z}} \operatorname{sinc}\left(l - \frac{m}{N}\right) \cdot \operatorname{sinc}\left(l - \frac{n}{N}\right)$. Using (11) and using that sinc is sampled at Nyquist rate in l we get

$$\begin{aligned} I_m[n] &= \left\langle \operatorname{sinc}\left(\cdot - \tfrac{m}{N}\right), \operatorname{sinc}\left(\cdot - \tfrac{n}{N}\right)\right\rangle_{\ell^2} \\ &= \left\langle \operatorname{sinc}\left(\cdot - \tfrac{m}{N}\right), \operatorname{sinc}\left(\cdot - \tfrac{n}{N}\right)\right\rangle_{L^2} = \operatorname{sinc}\left(\tfrac{n-m}{N}\right). \end{aligned}$$

Therefore we get the final expression

$$\psi_k[n] = \tfrac{1}{N}\sum\nolimits_{m=n_k+1}^{n_{k+1}} \operatorname{sinc}\left(\tfrac{n-m}{N}\right). \tag{14}$$

Sequence g is uniquely represented in ℓ_N^2 by coefficients $d_k/T = \langle g, \mathbb{1}_{[n_k+1,n_{k+1}]}\rangle_{\ell^2} = \langle g, \psi_k\rangle_{\ell^2}$, if ψ_k form a frame for ℓ_N^2. This is true if $\exists A_N, B_N > 0$ such that [23]

$$A_N\|g\|_{\ell^2}^2 \leqslant \sum\nolimits_{k\in\mathbb{Z}} \left|\langle g, \psi_k\rangle_{\ell^2}\right|^2 \leqslant B_N\|g\|_{\ell^2}^2, \quad \forall g \in \ell_N^2. \tag{15}$$

We note that

$$\langle g, \psi_k\rangle_{\ell^2} = \sum\nolimits_{l=n_k+1}^{n_{k+1}} g^c\left(\tfrac{l}{N}\right) = \Delta n_k \cdot g^c(\tau_k),$$

where $\tau_k \in [(n_k+1)T, n_{k+1}T]$. The above is true because $\frac{1}{\Delta n_k}\sum_{l=n_k+1}^{n_{k+1}} g^c\left(\frac{l}{N}\right)$ is an average of samples of g^c which is in between its minimum and maximum over interval $[(n_k+1)T, n_{k+1}T]$. Due to continuity, this value is always attained in some intermediate point τ_k. According to [24] (Th. 5), $g^c(t)$ is uniquely represented by samples $g^c(\tau_k)$, and thus $\{\operatorname{sinc}(t-\tau_k)\}_{k\in\mathbb{Z}}$ is a frame for PW_π, provided that $\sup(\tau_{k+1} - \tau_k) < 1$. From the property of τ_k, we have that

$$|\tau_{k+1} - \tau_k| \leqslant \tfrac{2}{N} \cdot \max|n_{k+1} - n_k| \leqslant \tfrac{4\delta}{b-c}, \tag{16}$$

where the last inequality is due to Lemma 1. Then, if $\frac{4\delta}{b-c} < 1$, we get the following frame conditions for $\{\operatorname{sinc}(t-\tau_k)\}_{k\in\mathbb{Z}}$

$$A\|g^c\|_{L^2}^2 \leqslant \sum\nolimits_{k\in\mathbb{Z}} |g^c(\tau_k)|^2 \leqslant B\|g^c\|_{L^2}^2. \tag{17}$$

Equivalently, using (11) and the definition of τ_k, we get

$$\frac{A}{N}\|g\|_{\ell^2}^2 \leqslant \sum\nolimits_{k\in\mathbb{Z}} \frac{|\langle g,\psi_k\rangle_{\ell^2}|^2}{|\Delta n_k|^2} \leqslant \frac{B}{N}\|g\|_{\ell^2}^2. \quad (18)$$

Finally using, Lemma 1, we get

$$\frac{A(b-c)}{\delta N}\|g\|_{\ell^2}^2 \leqslant \sum\nolimits_{k\in\mathbb{Z}} |\langle g,\psi_k\rangle_{\ell^2}|^2 \leqslant \frac{B(b+c)}{\delta N}\|g\|_{\ell^2}^2.$$

Then ψ_k is a frame with bounds $A_N = \frac{A(b-c)}{\delta N}$ and $B_N = \frac{A(b+c)}{\delta N}$, and thus g is uniquely identified by its samples $d_k = \langle g,\psi_k\rangle_{\ell^2}, k\in\mathbb{Z}$. Given that $g[l]$ are acquired at more than the Nyquist rate then they uniquely identify $g^c(t)$. □

Using that $g[l]$ can be expressed using the basis in ℓ_N^2 as $g[l] = \sum_{n\in\mathbb{Z}} c_n h_n[l]$ (10), the following holds

$$\sum_{n\in\mathbb{Z}} c_n T \sum_{l=n_k+1}^{n_{k+1}} h_n[l] = 2(-1)^k\delta + T\sum_{l=n_k+1}^{n_{k+1}-1} x[l] + \varepsilon_k, \quad (19)$$

where $\varepsilon_k \triangleq y[n_{k+1}] - y[n_k] - 2(-1)^k\delta$, $|\varepsilon_k| \leqslant 2T(b+c)$, is an unknown noise sequence. We note that the noise on the RHS can be made smaller by writing an equivalent system via cummulative sumation of the equations above (also see (5))

$$\sum\nolimits_{n\in\mathbb{Z}} c_n T \sum\nolimits_{l=0}^{n_k} h_n[l] = (-1)^{k+1}\delta + T\sum\nolimits_{l=0}^{n_k-1} x[l] + \overline{\varepsilon}_k, \quad (20)$$

where $\overline{\varepsilon}_k = y[n_k] - (-1)^{k+1}\delta$, $|\overline{\varepsilon}_k| < T(b+c)$. We note that $\overline{\varepsilon}_k = \delta + \sum_{l=0}^k \varepsilon_l$. Recovering the input amounts to computing $\{c_k\}$. We note that the RHS in (20) is known up to precision $\overline{\varepsilon}_k$ and, in reality, one assumes $\overline{\varepsilon}_k \simeq 0$ by solving

$$\widetilde{\mathbf{c}} = \mathbf{H}^+\mathbf{d}, \quad (21)$$

where $\mathbf{H}^+$ is the Moore-Penrose pseudoinverse of $\mathbf{H}$, $[\mathbf{H}]_{kn} = \sum_{l=n_k+1}^{n_{k+1}} h_n[l]$, and $[\mathbf{d}]_k = (-1)^{k+1}\delta + T\sum_{l=0}^{n_k-1} x[l]$.

A. Comparison with Conventional Quantization

The recovery for conventional quantization is achieved via (3) which, in practice is done by discretising the integral, which leads to a system similar to (19), only for a much smaller $\overline{T} \ll T$. That is why, in practice, the algorithm for recovering the input of the QTEM is the same as for a TEM with a quantized output. However, the QTEM can achieve much smaller recovery errors, as will be explained next. We note that (3) holds true with an error evaluated below

$$\sum_{n\in\mathbb{Z}} c_n \int_{t_k^q}^{t_{k+1}^q} \operatorname{sinc}(t-n)\,dt = (-1)^k\left[2\delta - b\Delta t_k^q\right] + \varepsilon_k^q, \quad (22)$$

with $\varepsilon_k^q \triangleq (-1)^k b\left(\Delta t_k - \Delta t_k^q\right) - \int_{t_k}^{t_k^q} g^c(s)ds - \int_{t_{k+1}^q}^{t_{k+1}} g^c(s)ds$. The error is bounded by $|\varepsilon_k^q| < bT + cT = T(b+c)$. If we attempt to design an equivalent system as in (20) via $\sum_{l=0}^k \varepsilon_k^q$, we note that this leads to an unbounded error, since $(-1)^k b\left(\Delta t_k - \Delta t_k^q\right)$ is a random variable whose summation leads to an unbounded random walk. This was also tested numerically, and an equivalent system as in (20) always led to significantly worse errors in the case of conventional quantization. However, this approach works very well for the recovery from QTEM data. In fact, the absolute error $|\overline{\varepsilon}_k| < T(b+c)$ satisfies the same bound as ε_k^q. However, as will be shown in the next section, this leads to a much smaller relative error, given that the RHS vector in (20) has a significantly higher norm than the RHS in (22) due to the cummulation process.

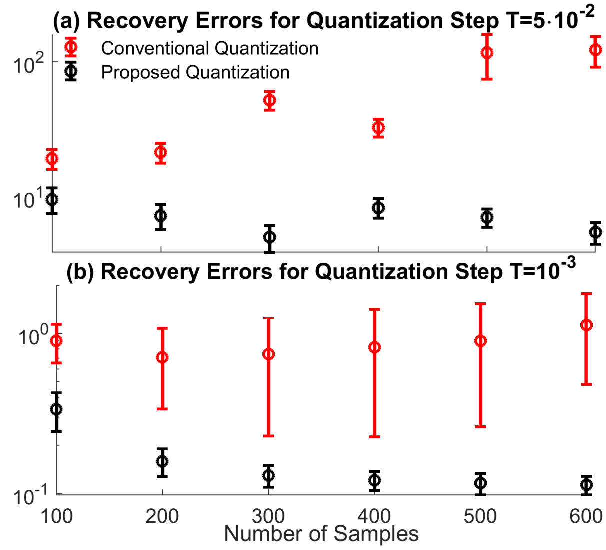

Figure 5: Comparative reconstruction performance for two levels of quantization and 6 different sample densities. The error bars show the mean and standard deviation computed for 100 inputs.

VI. Numerical Study

The input was generated using random coefficients $\{c_n\}$ drawn from the uniform distribution $U([-0.6, 0.6])$ as

$$g^c(t) = \sum_{n=-10}^{10} c_n \operatorname{sinc}(t-n), \quad t\in[-20,20]. \quad (23)$$

An ASDM TEM with parameters $\delta = 0.04, b = 1$ generated output samples $\{t_k\}_{k=1}^{466}$ in response to input $g^c(t)$. In the conventional quantization setting, these samples were quantized via $t_k^q = T\cdot\operatorname{round}\left(\frac{t_k}{T}\right)$ for quantization resolution $T = 5\cdot 10^{-2}$ s. The recovery $\widetilde{g}_1[k]$ via (3) is illustrated in Fig. 1, and resulted in error $\mathsf{Err}_1 = 100\cdot\frac{\|g-\widetilde{g}\|_{\ell^2}}{\|g\|_{\ell^2}} = 20.2\%$. The same input was used to test the proposed QTEM method. Given that generally the number of output samples is different from the TEM, for comparison purposes, for $b = 1$, the value of δ was automatically tuned until the QTEM generated roughly the same number of samples, namely $\{t_k^{q_2}\}_{k=1}^{467}$, for $\overline{\delta} = 0.019$. The input reconstructed via (20) is depicted in Fig. 1(b), and resulted in error $\mathsf{Err}_2 = 6.9\%$. To further evaluate the proposed method, 100 inputs were randomly generated via (23) and encoded with both methods using $T = 50$ ms and $b = 1$ for 6 different target numbers of samples uniformly distributed within $[100, 600]$. Parameters $\delta, \overline{\delta}$ were subsequently automatically adjusted for TEM and QTEM, to achieve the target number of samples with a 1% accuracy. The experiment was repeated for $T = 1$ ms. The results, depicted in Fig. 5, show that the proposed method is around an order of magnitude more accurate, and the difference increases for larger number of samples and higher T.

VII. Conclusions

In this work we introduced a new model-driven quantization method for time encoding machines (TEMs) called QTEM. We formulate the recovery problem in frame theory and introduce recovery guarantees. Using extensive numerical simulations, we showed that the proposed method leads to around one order of magnitude smaller errors than conventional TEM quantization. The simulations show that QTEM enables to a better degree the quantization/sampling trade-off from conventional ADCs, where a higher sampling rate can tackle more quantization noise.

References

[1] B. Widrow, I. Kollar, and M.-C. Liu, "Statistical theory of quantization," *IEEE Trans. Instrum. Meas.*, vol. 45, no. 2, pp. 353–361, 1996.

[2] A. A. Lazar and L. T. Tóth, "Perfect recovery and sensitivity analysis of time encoded bandlimited signals," *IEEE Trans. Circuits Syst. I*, vol. 51, no. 10, pp. 2060–2073, 2004.

[3] A. A. Lazar and E. A. Pnevmatikakis, "Faithful representation of stimuli with a population of integrate-and-fire neurons," *Neural computation*, vol. 20, no. 11, pp. 2715–2744, 2008.

[4] D. Florescu and D. Coca, "A novel reconstruction framework for time-encoded signals with integrate-and-fire neurons," *Neural computation*, vol. 27, no. 9, pp. 1872–1898, 2015.

[5] D. Gontier and M. Vetterli, "Sampling based on timing: Time encoding machines on shift-invariant subspaces," *Appl. Comput. Harmon. Anal.*, vol. 36, no. 1, pp. 63–78, 2014.

[6] D. Florescu and A. Bhandari, "Time encoding via unlimited sampling: Theory, algorithms and hardware validation," *IEEE Trans. Sig. Proc.*, vol. 70, pp. 4912–4924, 2022.

[7] D. Florescu, F. Krahmer, and A. Bhandari, "Event-driven modulo sampling," in *IEEE Intl. Conf. on Acoustics, Speech and Sig. Proc. (ICASSP)*, 2021, pp. 5435–5439.

[8] D. Florescu and A. Bhandari, "Modulo event-driven sampling: System identification and hardware experiments," in *ICASSP 2022-2022 IEEE International Conference on Acoustics, Speech and Signal Processing (ICASSP)*. IEEE, 2022, pp. 5747–5751.

[9] K. Adam, A. Scholefield, and M. Vetterli, "Sampling and reconstruction of bandlimited signals with multi-channel time encoding," *IEEE Transactions on Signal Processing*, vol. 68, pp. 1105–1119, 2020.

[10] N. T. Thao and D. Rzepka, "Time encoding of bandlimited signals: Reconstruction by pseudo-inversion and time-varying multiplierless fir filtering," *IEEE Transactions on Signal Processing*, vol. 69, pp. 341–356, 2020.

[11] D. Chklovskii and D. Soudry, "Neuronal spike generation mechanism as an oversampling, noise-shaping A-to-D converter," *Advances in Neural Information Processing Systems*, vol. 25, 2012.

[12] M. Miśkowicz, *Event-based control and signal processing*. CRC press, 2018.

[13] H. Naaman, S. Mulleti, and Y. Eldar, "Time-based quantization for fri and bandlimited signals," in *European Sig. Proc. Conf. (EUSIPCO)*, 2022, pp. 2241–2245.

[14] E. Doutsi, L. Fillatre, M. Antonini, and P. Tsakalides, "Dynamic image quantization using leaky integrate-and-fire neurons," *IEEE Transactions on Image Processing*, vol. 30, pp. 4305–4315, 2021.

[15] N. T. Thao, D. Rzepka, and M. Miśkowicz, "Bandlimited signal reconstruction from leaky integrate-and-fire encoding using POCS," *IEEE Transactions on Signal Processing*, 2023.

[16] D. Kościelnik and M. Miśkowicz, "Asynchronous sigma-delta analog-to digital converter based on the charge pump integrator," *Analog Integrated Circuits and Signal Processing*, vol. 55, pp. 223–238, 2008.

[17] D. Rzepka, D. Kościelnik, J. Szyduczyński, M. Pawlak, and M. Miśkowicz, "Recovery of signals encoded by sample-and-hold asynchronous sigma-delta modulation," in *2018 IEEE International Conference on the Science of Electrical Engineering in Israel (ICSEE)*, 2018, pp. 1–5.

[18] A. Rybakov, "The use of asynchronous sigma-delta modulation in analog-signal sampling based on event-timing techniques," *Automatic Control and Computer Sciences*, vol. 50, no. 6, pp. 385–396, 2016.

[19] E. Roza, "Analog-to-digital conversion via duty-cycle modulation," *IEEE Trans. Circuits Syst. II*, vol. 44, no. 11, pp. 907–914, 1997.

[20] K. Ozols, "Implementation of reception and real-time decoding of ASDM encoded and wirelessly transmitted signals," in *25th International Conference Radioelektronika*, 2015, pp. 236–239.

[21] D. Wei, V. Garg, and J. G. Harris, "An asynchronous delta-sigma converter implementation," in *IEEE Intl. Symposium on Circuits and Systems*, 2006, pp. 4903–4906.

[22] K. Ozols, M. Greitans, and R. Shavelis, "EEG data acquisition system based on asynchronous sigma-delta modulator," in *Biennial Baltic Electronics Conf.*, 2012, pp. 183–186.

[23] O. Christensen *et al.*, *An introduction to frames and Riesz bases*. Springer, 2003, vol. 7.

[24] H. Feichtinger, "Theory and practice of irregular sampling," *Wavelets: Math. and Appl.*, 1993.